Available online at www.sciencedirect.com
SCIENCE DIRECT®
Nuclear Instruments and Methods in Physics Research A 560 (2006) 93–97
NUCLEAR INSTRUMENTS & METHODS IN PHYSICS RESEARCH Section A
www.elsevier.com/locate/nima

Radiation hardness studies of silicon pixel detectors

T. Lari

INFN and Università di Milano, Dipartimento di Fisica, Via Celoria 16, I-20133 Milano, Italy

Available online 28 December 2005

Abstract

At the LHC silicon vertex detectors will be exposed to hadron fluences of the order of $10^{15}\,n_{eq}\,cm^{-2}$. In order to study the effects of radiation damage on the performances of the ATLAS Pixel Vertex Detector, several full-size detector modules were irradiated to a fluence of $1.1\times10^{15}\,n_{eq}\,cm^{-2}$ and tested in a beam at CERN. After irradiation only a modest degradation of the detector performances is observed. At the operating ATLAS bias voltage of 600 V the average signal is still 80% of the pre-irradiation value, the spatial resolution is 9.6 μm and the detection efficiency is 98.2%. The LHC luminosity upgrade will increase the radiation hardness requirements by a factor of 10 and will require the development of new ultra-radiation hard vertex detectors. A detailed simulation of silicon pixel detectors irradiated to very high fluence is presented and used to study the possibility to use silicon pixel detectors at the LHC after the luminosity upgrade. The charge collection properties and the detector response were computed for different silicon materials (Standard Float Zone, Diffusion Oxygenated Float Zone, Czochralski, epitaxial silicon) and operating conditions (bias voltage, temperature). At the maximum fluence ($10^{16}\,n_{eq}\,cm^{-2}$) the signal is limited by charge trapping rather than by the thickness of the active volume. Since all the silicon materials studied so far have a similar trapping cross-section, they are all expected to collect an average signal of 2000–2500 electrons at 600 V bias voltage. A detection threshold of 1000–1200 electrons is required in order to have a 97% detection efficiency.

PACS: 29.40.Gx; 07.89.+b

Keywords: Pixel detector; Radiation damage; ATLAS; LHC upgrade

1. Introduction

When the Large Hadron Collider (LHC) will operate at the design luminosity of $10^{34}\,cm^{-2}\,s^{-1}$ the innermost layers of the vertex detectors will be exposed to charged hadron fluences[1] of about $3\times10^{14}\,n_{eq}\,cm^{-2}\,year^{-1}$ [1]. In order to study the effects of radiation damage on the performances of the ATLAS Pixel detector, several full-size detector modules (sensor and electronics) were irradiated to a fluence of $1.1\times10^{15}\,n_{eq}\,cm^{-2}$ and tested with a pion beam at CERN. A detailed study of their performances is presented in Section 3. Measurements of the thickness of the depleted depth, charge collection efficiency, trapping lifetime, spatial resolution and particle detection efficiency are discussed.

The proposed LHC luminosity upgrade [2] would increase the luminosity and the radiation hardness requirements by a factor of 10. New vertex detectors will be required to maintain the vertexing performances of the experiments. The CERN RD50 collaboration is developing silicon sensors with increased radiation hardness [3]. Oxygen-rich silicon substrates (diffusion oxygenated, Czochralski and epitaxial sensors) have been found to be more radiation tolerant than conventional float-zone (FZ) silicon [3,4]. In order to study the performances expected by detectors using these materials after irradiation to very high fluences, a simulation of the detection of ionizing radiation with irradiated pixel detectors has been developed. The simulation is described in Section 4. In Section 5 the performance of pixel silicon detectors is computed after irradiation to the fluences expected after the LHC luminosity upgrade, up to $10^{16}\,n_{eq}\,cm^{-2}$. A detailed study of the collected charge and detection efficiency is presented for different sensor materials (standard FZ, Diffusion Oxygenated Float Zone (DOFZ), Czochralski and

E-mail address: lari@mi.infn.it.

[1]Fluences are expressed in the equivalent fluence of 1 MeV neutrons with the same non-ionizing energy loss.

0168-9002/$ - see front matter © 2005 Elsevier B.V. All rights reserved.
doi:10.1016/j.nima.2005.11.227

epitaxial silicon) as a function of the operating conditions (bias voltage, temperature, electronics threshold).

2. Radiation damage in silicon sensors

The main effects of radiation damage on macroscopic silicon sensor properties are [5,6]:

- An increase of leakage current, which can be reduced by cooling.
- Increase of the space charge concentration N_{eff} in depleted silicon. This increases the bias voltage needed to achieve a given active thickness.
- Decrease of charge drift lifetime τ, which reduces the charge collection efficiency from the depleted region.

The second effect can be moderated by using oxygen-rich silicon substrates, like DOFZ silicon [4], already used for the ATLAS Pixel sensors [7–9], high resistivity Czochralski grown wafers [3,10] and epitaxial sensors [3,11].

The irradiation introduces an excess of acceptor centers in oxygenated and not-oxygenated FZ silicon. Heavily irradiated FZ silicon has thus a negative space charge concentration regardless of the sign of the initial doping concentration and it requires n-side readout for better performances [12,13]. In Czochralski wafers, instead, the irradiation introduces an excess of donor centers allowing the use of cheaper p-on-n technology. Thin (50 μm) epitaxial diodes show very little variation of the space charge concentration with fluence. Detectors using this material may be operated completely depleted up to the upgraded LHC fluences.

The space charge concentration also varies with time because of the thermal annealing of defects. It decreases to a minimum after about one week at room temperature, then it increases again [3,6].

3. ATLAS Pixel detector test-beam results

An ATLAS Pixel detector module [9,14] is composed of an n^+/n diffusion oxygenated silicon sensor [7], 16 readout electronics chips using 0.25 μm deep-submicrometer rad-hard technology [15,16], and a flexible hybrid supporting a module controller chip [17], signal interconnection and power distribution lines and passive components such as temperature sensors, resistors and capacitors. The sensor has a size of $16.4 \times 60.8\,\mathrm{mm}^2$ and a thickness of 250 μm. The pixel implants have a pitch of $50 \times 400\,\mu\mathrm{m}^2$ and are connected via bump-bonding to matching cells in the readout chip, each featuring an electronics chain. A 7-bit charge measurement capability is provided. Each module use one of two bump-bonding technologies (solder or indium bonds [18]).

The performance of these modules have been tested using a 180 GeV/c pion beam. Several modules were irradiated before operation at the test-beam with 24 GeV/c protons. The proton fluence was $2 \times 10^{15}\,\mathrm{cm}^{-2}$, corresponding to $1.1 \times 10^{15}\,\mathrm{n_{eq}\,cm^{-2}}$. During irradiation, subsequent storage and test-beam operation the modules were kept at or below −5 °C. Several smaller sensors bump-bonded to single readout chip were also irradiated and studied at the test beam. These were studied after two different thermal annealing scenarios: a moderate annealing, corresponding to the minimum possible value of the full depletion voltage for a given fluence, and an annealing of 25 h at 60 °C, equivalent to the annealing expected during 5 years of detector operation at the LHC. The measurements of charge collection efficiency, the depleted depth and the trapping lifetime presented here were performed with the single chip assemblies while the measurement of efficiency was performed with full-size modules.

The test-beam setup included a beam telescope [19] of four double-sided microstrip planes which determined the particles' incident position on the plane of the pixel detector with a resolution of 6 μm. The time of the particles with respect to the edge of the 40 MHz clock operating the detectors was measured by a scintillator. Unless otherwise specified the irradiated modules were operated at 600 V.

The average charge collected after irradiation was $(72 \pm 14)\%$ and $(87 \pm 14)\%$ of the pre-irradiation value after moderate and end-of-lifetime annealing, respectively [8,20]. The error comes from the uncertainty on the absolute scale provided by charge calibrations. The depleted depth was measured using data taken with an angle of 30° between the beam direction and the normal to the sensor plane. The depleted depth was extracted from the distribution of the depth of the track segments subtended by the pixels which give a signal, as described in Ref. [21]. At 600 V bias voltage the full sensor thickness was depleted even after end-of-lifetime annealing [8].

The charge trapping due to irradiation was measured considering the dependence of the collected charge on the depth of the track segment subtended by a pixel (Fig. 1). The effect of charge trapping is evident in the irradiated sensors and it is less severe after the longer end-of-lifetime annealing, in agreement with the measurements of charge collection efficiency. The lifetime τ can be extracted assuming equal hole and electron lifetime and comparing the experimental distribution with the predictions of the simulation described in the next section. This procedure [20,22] gives $\tau = (2.3 \pm 0.2 \pm 0.8)\,\mathrm{ns}$ and $\tau = (4.1 \pm 0.2 \pm 0.6)\,\mathrm{ns}$ after moderate and end-of-lifetime annealing, respectively.

The spatial resolution of the detectors along the short dimension of the pixels ($R\phi$ in ATLAS) and at 10° incidence angle was measured to be 6.8 μm for not irradiated detectors and 9.6 μm for detectors irradiated to $1.1 \times 10^{15}\,\mathrm{n_{eq}\,cm^{-2}}$. A charge interpolation algorithm, described in Ref. [21], was used. The extrapolation uncertainty of about 6 μm of the beam telescope was not subtracted.

The efficiency to detect a particle in a 25 ns clock period (in-time efficiency) was measured as a function of the

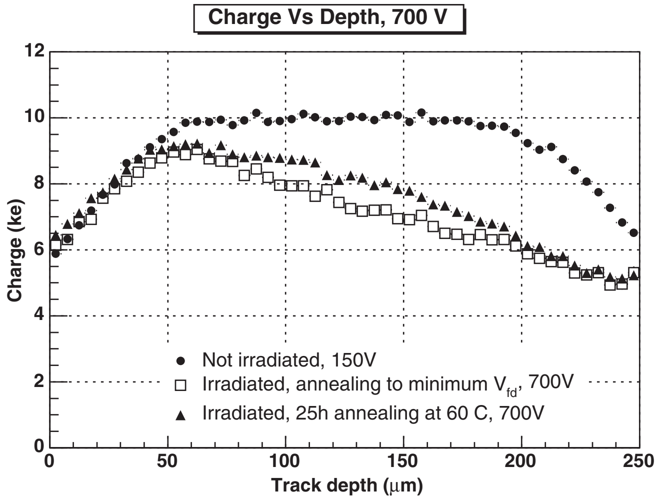

Fig. 1. Charge collected by a pixel as a function of the average depth of subtended track segment. The curve is shown for a not irradiated detector, and two detectors irradiated to $1.1 \times 10^{15}\,\mathrm{n_{eq}\,cm^{-2}}$. The irradiated detectors were distinguished by the different annealing scenarios as explained in the text. The charge collected by each detector is subject to a 10% systematic error because of the uncertainty on the normalization scale provided by charge calibrations.

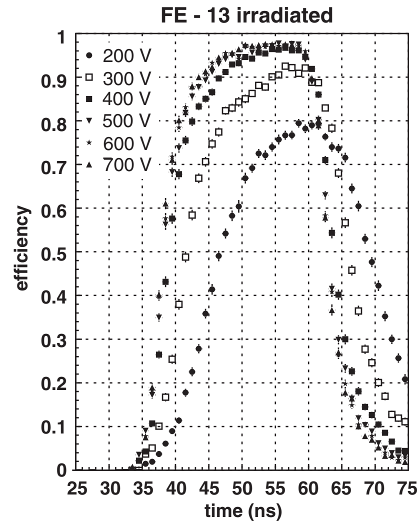

Fig. 2. Variation of detection efficiency with operating bias voltage for an ATLAS Pixel detector irradiated to $1.1 \times 10^{15}\,\mathrm{n_{eq}\,cm^{-2}}$ fluence. On the x-axis there is the difference between the arrival time of the particles and the clock edge.

difference between the arrival time of the particles and the clock edge. The efficiency curve is reported in Fig. 2 for an irradiated module and for several different bias voltages. The maximum efficiency is achieved as soon as the sensor is fully depleted at 500 V. Since in ATLAS it will be possible to tune the phase of the clock, the maximum of the curve is the quantity of interest. Typical values for the in-time efficiency are 99.8% before irradiation and 98.2% after irradiation.

4. Simulation of irradiated detectors

The simulation used to compute silicon detector performances after irradiation is described in detail in [23]. The interactions of ionizing radiation with the silicon sensors are simulated with the Geant4 software [24]. The resulting charges are drifted in silicon until they are trapped or collected by an electrode. Dependence of drift velocity and diffusion on local electric field and temperature is parametrized as in Ref. [25]. Signal induction on the electrodes is computed with the weighting field formalism [26,27]. Readout electronics effects (noise, threshold, cross-talk) are finally taken into account. ATLAS Pixel test beam data, taken with irradiated and not irradiated detectors, were used to validate the simulation. A good agreement was found between the simulated results and experimental data [23].

Radiation damage effects were simulated using parameterizations of the variation of full depletion voltage and charge lifetime before trapping as a function of equivalent neutron fluence Φ. The full depletion voltage was computed using a uniform space charge concentration parametrized as a function of fluence as $N_{\mathrm{eff}} = g\Phi$ with $g = 0.0022\,\mathrm{cm^{-1}}$ for not-oxygenated silicon, $g = 0.009\,\mathrm{cm^{-1}}$ for DOFZ, and $g = -0.009\,\mathrm{cm^{-1}}$ for Czochralski. These parameterizations are valid for charged hadron irradiation, which is appropriate to simulate the effects of radiation damage at the LHC for the inner parts of the trackers, where the fluence will be dominated by charged particles. They also assume a thermal annealing to the minimum of full depletion voltage. A constant value (i.e. independent of fluence) of $N_{\mathrm{eff}} = 1.32 \times 10^{13}\,\mathrm{cm^{-3}}$, corresponding to a depleted thickness of $50\,\mu\mathrm{m}$ at 100 V bias voltage, was used for epitaxial silicon.[2]

The lifetime before trapping was computed for all materials as $\tau = 1/\beta\Phi$, with $\beta_{\mathrm{e}} = 5 \times 10^{-16}(T/263\,\mathrm{K})^{-0.86}\,\mathrm{cm^2\,s^{-1}}$ for electrons and $\beta_{\mathrm{h}} = 5 \times 10^{-16}(T/263\,\mathrm{K})^{-1.52}\,\mathrm{cm^2\,s^{-1}}$ for holes [3,28]. Since the lifetime is proportional to $1/\Phi$, while the depleted depth is proportional to $1/\sqrt{\Phi}$, the signal at very high fluences is limited by charge trapping.

For the radiation hardness study of new silicon pixel detectors reported here [29], four types of material have been considered: standard float zone (StFZ), diffusion oxygenated (DOFZ), Czochralski and epitaxial. Readout is on the side with maximum electric field after irradiation (n-side for StFZ and DOFZ, p-side for Czochralski and epitaxial silicon). Unless otherwise specified, the following parameters have been used. The pixel pitch is $70 \times 70\,\mu\mathrm{m}^2$ smaller than the one of present ATLAS and CMS detectors to cope with the increased track density. The thickness is $250\,\mu\mathrm{m}$ for StFZ, DOFZ and Czochralski sensors and $50\,\mu\mathrm{m}$ for epitaxial detectors. The operating bias voltage is 150 V for the thin epitaxial detectors, and 600 V for

[2]This is a typical value for the first samples of epitaxial sensors studied by the RD50 collaboration [11].

irradiated StFZ, DOFZ and Czochralski detectors. Temperature is −10 °C.

5. Simulation results

Collected charge as a function of radiation fluence. In Fig. 3 the sum of the positive signals induced on the pixels is reported as a function of fluence.[3] Epitaxial detectors have a signal limited by their thickness. It gradually decreases because of trapping. At intermediate fluences the DOFZ and Czochralski detectors give the larger charge because of their larger depleted depth. At a fluence of $10^{16}\,n_{eq}\,cm^{-2}$ the difference between the considered materials becomes small, since the collected charge is limited by the trapping mean free path, which is lower than the depleted depth and it is the same for all materials.

Collected charge as a function of bias voltage. In Fig. 4 the collected charge is reported after $10^{16}\,n_{eq}\,cm^{-2}$ as a function of bias voltage, for 250 μm thick DOFZ and Czochralski detectors (full depletion voltage 4200 V) and a 50 μm thick epitaxial detector (full depletion voltage 100 V). The epitaxial detector is still completely depleted at 100 V, but a larger bias voltage is required to reach the maximum value of collected charge (about 2500 electrons). This occurs when the electric field is strong enough that the electron and hole drift velocities reach their saturation value everywhere in the sensor. For the partially depleted DOFZ and Czochralski detectors a more gradual flattening of the dependence of charge on bias voltage is predicted. At 600 V the signal collected by DOFZ and Czochralski detectors is comparable to the one collected by the epitaxial sensor.

Dependence of collected charge on the thickness of the epitaxial sensors. The signal expected from epitaxial sensors of different thickness was computed for three different values of the sensor thickness (50, 75 and 100 μm). A constant doping concentration of $N_{eff} = 1.32 \times 10^{13}\,cm^{-3}$ is assumed, so that the values of the full depletion voltage V_{fd} are 100, 225 and 400 V. When the bias voltage exceeds the full depletion voltage the thicker sensor collects a larger signal, but the advantage of the additional active thickness is limited by charge trapping. At a bias voltage of 600 V, the average signal increases from $2400e^{-}$ to $2900e^{-}$ when the thickness is increased from 50 to 100 μm.

Dependence of collected charge on the operating temperature. The collected charge is predicted to have only a very weak dependence on temperature in the range between 200 and 300 K, since the increase of the electron and hole mobilities at lower temperature is compensated by the shorter trapping time. The charge collected after $10^{16}\,n_{eq}\,cm^{-2}$ increases by about 5% if the temperature is increased from 223 to 283 K.

Collection time. The collection time decreases with fluence for both DOFZ (n-side readout) and Czochralski (p-side readout) because of the reduction of the thickness of the depleted depth, the increase of the electric field and the short trapping times. It is well below 1 ns after a fluence of $10^{16}\,n_{eq}\,cm^{-2}$. The same conclusion holds for 50 μm epitaxial detectors at all fluences, because of their small thickness.

Electronics threshold and detection efficiency. The detection efficiency expected for a DOFZ sensor irradiated to $10^{16}\,n_{eq}\,cm^{-2}$ and operated at 600 V is reported in Fig. 5 as a function of the threshold. The efficiency is reported for three different particle incident angles, but since at these fluences the mean free path of charges before trapping is only about 20 μm, the sharing of the ionization charge between pixels is limited and the efficiency does not strongly depend on the incident angle. In order to achieve 97% efficiency at a fluence of $10^{16}\,n_{eq}\,cm^{-2}$, a threshold of 1000–1200 electrons is required. A noise and time-walk performance compatible with operation at these thresholds is the requirement that the currently available sensors place on the electronics.

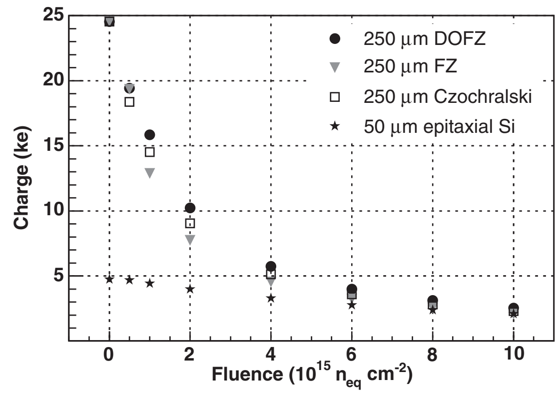

Fig. 3. Average collected charge as a function of fluence, for different types of silicon pixel detectors. The operating bias voltage is 600 V.

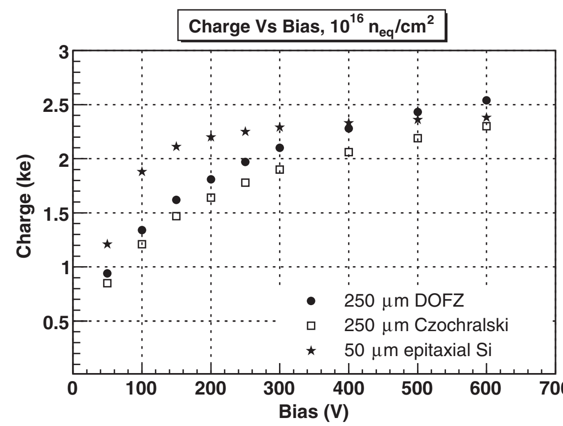

Fig. 4. Average charge collected after a fluence of $10^{16}\,n_{eq}\,cm^{-2}$ as a function of bias voltage, for 250 μm thick DOFZ and Czochralski detectors (full depletion voltage 4240 V) and a 50 μm thick epitaxial detector (full depletion voltage 100 V).

[3] The average of the charge distribution, computed between 0 and 100 000 electrons, is reported.

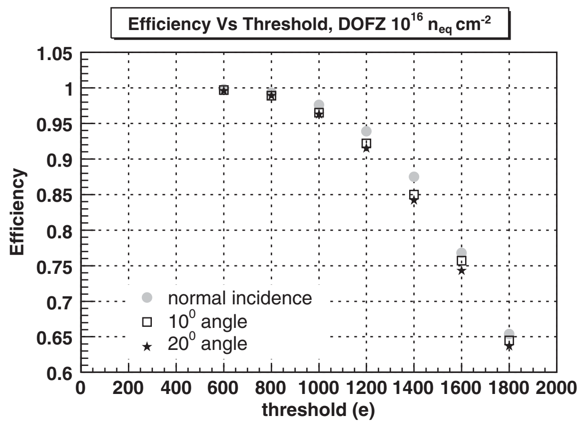

Fig. 5. Detection efficiency as a function of the threshold, for a DOFZ detector irradiated to $10^{16}\,n_{eq}\,cm^{-2}$. The different marker sets correspond to three different values of the particle incident angle.

6. Conclusions

A test-beam study of ATLAS Pixel detectors irradiated to $1.1 \times 10^{15}\,n_{eq}\,cm^{-2}$ was presented. The charge collection properties of the sensors were very satisfactory. The 250 μm thick detectors are almost fully depleted at the ATLAS standard operating bias voltage of 600 V and the average signal was equal to $(87 \pm 14)\%$ of the pre-irradiation value. A spatial resolution of 9.6 μm and an in-time detection efficiency of 98.2% were achieved after irradiation.

In order to study the feasibility of using silicon vertex detectors at the LHC even after the luminosity upgrade, a detailed simulation of the operation of irradiated silicon pixel detectors was developed to determine the performance of devices using the newest rad-hard silicon materials after $10^{16}\,n_{eq}\,cm^{-2}$. An average signal of 2000–2500 electrons is foreseen for detectors operated at 600 V. At this fluence little difference is expected between standard float-zone silicon and the different types of oxygenated silicon investigated (diffusion oxygenated, Czochralski, epitaxial), since the signal is limited by charge trapping rather than by the thickness of the depleted region. Only small variations of the charge collection efficiency are expected from different operation conditions and detector geometries.

The detection efficiency after irradiation to $10^{16}\,n_{eq}\,cm^{-2}$ fluence was studied as a function of detection threshold. High-efficiency operation requires low-noise and rad-hard readout electronics, capable of operating with a threshold of 1000–1200 electrons.

Acknowledgements

The test-beam results are the product of a collaboration-wide effort of the ATLAS Pixel group. The simulation studies have been done in the framework of RD50 collaboration activities.

References

[1] The ATLAS Inner Detector Collaboration, Inner Detector Technical Design Report, CERN/LHCC 97-17, 1997.
[2] F. Gianotti et al., Physics potential and experimental challenges of the LHC luminosity upgrade, hep-ph/0204087, 2002.
[3] RD50 Collaboration status report, CERN-LHCC-2003-058.
[4] G. Lindström, et al., Nucl. Instr. and Meth. A 466 (2001) 308.
[5] R. Wunstorf, IEEE Trans. Nucl. Sci. NS-44 (1997) 406.
[6] G. Lindström, et al., Nucl. Instr. and Meth. A 426 (1999) 1.
[7] I. Gorelov, et al., Nucl. Instr. and Meth. A 489 (2002) 202.
[8] C. Troncon, Nucl. Instr. and Meth. A 530 (2004) 65.
[9] A. Andreazza, Nucl. Instr. and Meth. A 535 (2004) 357.
[10] J. Harkonen, et al., Nucl. Instr. and Meth. A 518 (2004) 224.
[11] G. Kramberger, et al., Nucl. Instr. and Meth. A 515 (2003) 665.
[12] T. Rohe, et al., Nucl. Instr. and Meth. A 409 (1998) 224.
[13] G. Casse, et al., Nucl. Instr. and Meth. A 511 (2003) 112.
[14] C. Gemme, these proceedings.
[15] E. Mandelli, et al., IEEE Trans. Nucl. Sci. NS-49 (2002) 1774.
[16] L. Blanquart, et al., IEEE Trans. Nucl. Sci. NS-49 (2002) 1778.
[17] R. Beccherle, et al., Nucl. Instr. and Meth. A 492 (2002) 117.
[18] L. Rossi, Nucl. Instr. and Meth. A 501 (2003) 239; N. Wermes, Nucl. Instr. and Meth. A 512 (2003) 277.
[19] J. Treis, et al., Nucl. Instr. and Meth. A 490 (2002) 112.
[20] T. Lari, Nucl. Instr. and Meth. A 518 (2004) 349.
[21] I. Gorelov, et al., Nucl. Instr. and Meth. A 481 (2002) 204.
[22] G. Alimonti, et al., A study of charge trapping in irradiated silicon with test beam data, ATLAS Internal Note, CERN/ATL-INDET-2003-014, 2003.
[23] T. Lari, A Geant4 simulation of not irradiated and irradiated pixel detectors, ATLAS Internal Note, CERN/ATL-INDET-2003-015, 2003.
[24] S. Agostinelli, et al., Nucl. Instr. and Meth. A 506 (2003) 250.
[25] C. Jacoboni, et al., Solid State Electron. 20 (1977) 77.
[26] S. Ramo, Proc. I.R.E. 27 (1939) 584.
[27] V. Radeka, et al., Ann. Rev. Nucl. Part. Sci. 38 (1988) 217.
[28] G. Kramberger, et al., Nucl. Instr. and Meth. A 481 (2002) 297.
[29] T. Lari, C. Troncon, Simulation of signals in ultra radiation-hard silicon pixel detectors, IEEE Trans. Nucl. Sci., to be published.